J. Biomater. Sci. Polymer Edn, Vol. 15, No. 2, pp. 215–227 (2004)

Also available online - www.vsppub.com

Controlling modulus and morphology of hydrogel tubes through surface modification

CRISTINA ENESCU [1] and MOLLY S. SHOICHET [1,2,3,*]

[1] *Department of Chemical Engineering and Applied Chemistry, University of Toronto, 200 College Street, Toronto, ON, Canada M5S 3E5*
[2] *Department of Chemistry, University of Toronto, 80 St. George Street, Toronto, ON, Canada M5S 3H6*
[3] *Institute of Biomaterials and Biomedical Engineering, University of Toronto, 4 Taddle Creek Road, Toronto, ON, Canada M5S 3G9*

Received 7 Yuly 2003; accepted 22 October 2003

Abstract—Crosslinked, porous poly(2-hydroxyethyl methacrylate-*co*-methyl methacrylate) (PHEMA-MMA) tubes were prepared in cylindrical glass molds using a new centrifugal casting process developed in our group. The resulting hydrogel tubes have a bi-phasic wall structure, with a spongy inner layer and a gel-like outer layer, the latter of which provides mechanical strength to the tube. While many factors influence wall morphology and, thus, mechanical properties, we focused on the effect of the surface properties of the glass mold in which tubes are synthesized. Specifically, we investigated the impact of a diverse set of silane modifications of the glass mold on tube morphology, elastic modulus and mold release. We treated activated glass surfaces with one of three alkoxysilanes having either ethoxy, amine or fluorocarbon end-groups. Silane-modified glass surfaces were found to be more hydrophobic than the unmodified glass mold, with the most hydrophobic surface being that of the fluorocarbon-terminated silane. The presence of the silane layer on the mold was confirmed by X-ray photoelectron spectroscopy and the stability of this modification was confirmed by examining the surface chemistry of the hydrogel tubes. The biphasic hydrogel tube wall structure was observed for all tubes, yet those tubes synthesized in unmodified molds had a cracked outer morphology, whereas those synthesized in silane-modified molds had a smooth outer morphology. This influenced the mechanical properties of the tubes where tubes synthesized in silane-modified molds had a significantly greater elastic modulus than those tubes synthesized in unmodified molds. Release from the molds was easiest with ethoxy- and amine-functionalized silane mold modifications.

Key words: Surface modification; tube wall structure; poly(2-hydroxyethyl methacrylate-*co*-methyl methacrylate); silane; mechanical properties.

*To whom correspondence should be addressed at the Department of Chemical Engineering and Applied Chemistry. Tel.: (1-416) 978-1460. Fax: (1-416) 978-4317. E-mail: molly@ecf.utoronto.ca

INTRODUCTION

Hydrogels have been used extensively in biomedical engineering [1–8], particularly for soft tissue applications, where the mechanical properties of the hydrogel can be tuned to match those of the tissue. We have taken advantage of this property with poly(2-hydroxyethyl methacrylate-*co*-methyl methacrylate) (PHEMA-MMA) crosslinked, porous hydrogel tubes for guided regeneration of both the peripheral nerve and spinal cord [4–6]. A new centrifugal casting process, that combines liquid–liquid phase separation with centrifugal forces in a tubular glass mold, results in tubes with controlled dimensions, permeability, wall morphology and thickness [7–9]. Tubes can have a biphasic wall morphology that consists of a spongy inner layer, which provides high porosity and greater surface area for tissue regeneration, and a gel-like outer layer, which provides mechanical strength. The latter is influenced by many parameters, including the concentration of MMA co-monomer in the formulation, where higher MMA concentrations yield greater gel phase in the wall and thus higher tube elastic moduli. We found that the surface chemistry of the mold also impacted the tube wall morphology and elastic modulus [8]. In order to create tubes with higher moduli, so as to maximize functional outcome *in vivo*, we investigated a series of different surface-modified molds.

The interface between the mold and the polymer tube can be modified by either changing the surface properties of the mold [10–14] or by supplementing the polymer formulation with an additive [15–18]. The latter method of modifying the interface with surface-active molecules has been investigated with small molecules and macromolecules for both coatings [19] and biomedical applications [20]. The former method of modifying the mold by, for example, adsorption or covalent bonding, has been examined with several reagents including, for example, silicone oils [10], aliphatic esters [11], siloxanes [12], silanes and fluorinated olefins [13].

We chose to modify our glass tubular molds with silanes because they have been extensively examined [21], are non-cytotoxic when immobilized and have been used to control cell adhesion [22]. Silanes have the generic formula, R_nSiX_{4-n}, where $n = 1, 2$, or 3, R is a non-hydrolyzable organic group and X a hydrolyzable group (often a halogen or an alkoxy group). Silanes are advantageous to use because (1) the mold's surface hydrophobicity can be tuned by the silane organofunctionality chosen, (2) pre-hydrolyzed silanes in aqueous solutions chemically bond to the glass surface and simultaneously polymerize to a three dimensional siloxane network, providing a stable layer for release purposes and (3) silane-modified glass surfaces are stable and unlikely to de-bond onto the tube. A potential disadvantage of silane modification is the difficulty in attaining reproducible results, which can be overcome, in part, by carefully cleaning and activating all glass surfaces prior to modification [22].

To gain greater insight into the utility of silane modification of glass molds to influence tube properties, we treated activated glass surfaces with one of three alkoxysilanes having either hydrocarbon, amine or fluorocarbon end-groups. We

hypothesized that the mold surface chemistry would influence tube-wall morphology and elastic modulus. We characterized mold surface properties by X-ray photoelectron spectroscopy (XPS) and dynamic water contact angle (Wilhelmy method) measurements and correlated these with tube mechanical properties and scanning electron microscopy (SEM) micrographs. The stability of the silane layer on the mold was examined by XPS analysis of hydrogel tubes synthesized in *un*-modified and silane surface-modified glass molds. To gain greater insight into the modification chemistry, glass coverslips were used as models for glass molds, facilitating XPS and contact angle analysis.

MATERIALS AND METHODS

Materials

All chemicals were purchased from Aldrich (Milwaukee, WI, USA) and used as received unless indicated otherwise. The alkoxysilanes were obtained from Gelest (Tullytown, PA, USA), stored in a dessicator before use and include: 2-methoxy-(polyethyleneoxy)propyl trimethoxysilane (PEOSi), N-(2-aminoethyl)-3-aminopropyl trimethoxysilane (AminoSi) and (tridecafluoro-1,1,2,2-tetrahydrooctyl) triethoxysilane (FluoroSi). Water was distilled and deionized using Millipore Milli-RO 10 Plus and Milli-Q UF Plus (Bedford, MA, USA) and used at 18 MΩ. Aqueous solutions of ammonium persulfate (APS) and sodium metabisulfite (SMBS) were used together as redox initiators and made prior to every use. Ethylene dimethacrylate (EDMA) was added as a crosslinking agent in all polymerizations.

Surface modification and characterization of glass

Activation of surface hydroxyl groups on glass coverslips and molds. Borosilicate glass coverslips (22 × 22 × 0.15 mm; Bellco, Vineland, NJ, USA) and molds (Kimble, Vineland, NJ, USA) were activated as previously described [22]. Briefly, glass coverslips and molds were cleaned by sonication in a Glass & Plastic Cleaner^{TM} 100 solution (Texwipe, Upper Saddle River, NJ, USA) for 10 min, rinsed thoroughly with deionized water and then air-dried for 30 min. The dry coverslips and molds were immersed for 15 min in a solution containing nine parts of concentrated sulfuric acid (BDH, Toronto, Ontario, Canada) and one part of 30 wt% hydrogen peroxide in water (BDH), rinsed repeatedly with water and then air-dried. Unmodified glass coverslip and molds that were cleaned and activated in this way served as controls.

Reaction of silanes with activated glass. The procedure for modifying glass surface chemistry was previously described [21, 23]. Briefly, all silanes were prepared at 2 wt% solutions, with PEOSi and AminoSi each in 95 wt% methanol/5 wt% water and FluoroSi in 2,2,2-trifluoroethanol. The PEOSi and FluoroSi solutions were

adjusted to pH 2 by adding concentrated hydrochloric acid (BDH). The activated coverslips and molds were immersed for 10 min in a warm silane solution (40°C), rinsed three times in the solvent in which the silane was dissolved (40°C), air-dried for 15 min and dried at 110°C for 30 min prior to analysis.

Characterization of surfaces. Glass coverslip surfaces were characterized by dynamic advancing (θ_a) and receding (θ_r) water contact angles using a K12 process tensiometer (Krüss, Charlotte, NC, USA) at an immersion depth in water of 8 mm using the Wilhelmy plate method ($n = 3$; average ± standard deviation) [8]. All samples, including surface-modified glass molds and hydrogel tubes, were analyzed by XPS using a Leybold LH Max 200 surface analysis system (Leybold, Cologne, Germany) at take-off angles between sample and detector of 20° and 90°. Prior to XPS analysis all hydrogel tubes were immersed in water for approx. 24 h and then freeze-dried. The following controls were used: unmodified glass coverslip, unmodified glass mold and hydrogel tube synthesized in an un-modified glass mold. An aluminum K_α X-ray source was employed at an operating pressure of $<10^{-8}$ Torr and excitation energy of 1486.6 eV. The spectra were corrected for charging (approx. 2–3 eV) by calibrating against the aliphatic carbon peak at 285.0 eV. The sampling area for all XPS experiments was 2×4 mm^2 and the depth of analysis was between 40 Å and 100 Å for XPS angles of 20° and 90°, respectively. Survey and low-resolution spectra were obtained by averaging over 5 scans using pass energies of 192 eV. The elemental composition was calculated from satellite-subtracted spectra, normalized for constant transmission using tabulated sensitivity factors previously calculated for the Leybold Max 200 system. Peak deconvolution was performed using a program supplied by Specslab.

Polymerization of tubes

PHEMA-MMA hydrogel tubes were synthesized by a new liquid-liquid centrifugal casting method, as previously described [8], in disposable cylindrical glass molds (Kimble) rotated along their longitudinal axis. The molds had an inner diameter (ID) of 3.4 mm, which defined the outer diameter (OD) of the tube, and were cut at a length of 10 cm. Briefly, 28.55 wt% HEMA and 4.45 wt% MMA (for a total monomer concentration of 33 wt%) were dissolved in an aqueous 15 wt% ethylene glycol solution to which EDMA, APS and SMBS aqueous solutions were added at 0.1, 0.5 and 0.4 wt% of the total monomer concentration, respectively. Prior to the addition of SMBS, the monomer solution was degassed for approx. 3 min under reduced pressure, purified by passing through a 0.45 μm PTFE syringe filter, and then injected into a sealed glass mold. The mold was mounted horizontally in a drill (Heildoph, Germany), spun at 2500 rpm and the polymerization proceeded for 6 h at room temperature. The same formulation was used for all non-modified and silane surface-modified glass molds.

Tube-wall dimensions and morphology

The inner and outer diameters of the hydrated tube (after attaining equilibrium water content) were measured using an image analysis system (stereomicroscope Leica MZ-6) at two 90° cross-sections per tube to assess concentricity. SEM was used to examine the hydrogel tube wall morphology, and the thickness of the gel and porous phases were measured. Since environmental SEM and SEM showed similar wall morphologies (unpublished data) we chose to use SEM for these studies. Tube-wall dimensions and gel thickness were statistically compared using one way ANOVA (SigmaStat for Windows). The hydrogels, after reaching equilibrium in water, were cut, immersed in water in an Eppendorf vial, frozen in liquid nitrogen and then dried for 24 h in a freeze-dryer. The dried hydrogels were mounted onto aluminum studs and sputter-coated with gold in a Polaron vapour deposition unit (Polaron, Watford, UK) at 15 mA for 60 s. The SEM analyses were performed on a Hitachi system (S570, Hitachi, Mountain View, CA, USA) at an accelerating voltage of 20 kV and a working distance of 15 mm.

Release of hydrogel tubes from glass molds

The release of hydrogel tubes from glass molds was qualitatively assessed by carefully and gradually removing hydrogel tubes from glass molds. Release was assessed for four tubes per mold type and scored as either difficult to release, moderately difficult or easy to release.

Mechanical properties of hydrogel tubes

The elastic (Young's) modulus of hydrogels prepared in un-modified and silane-modified glass molds was determined as previously described [8], using a micro-mechanical tester (Dynatec Dalta Scientific Instruments, Galena, MO, USA). Briefly, after reaching equilibrium in water, samples of approx. 25 mm in length underwent a tensile test at a pulling rate of 0.5%/s. The applied force and resulting deformations were collected using LabView 4.0 data acquisition software (National Instruments, Austin, TX, USA) through an AT-MIO-16E-E serial interface (National Instruments). The following equation was employed to calculate the elastic modulus:

$$E = \frac{\sigma}{\varepsilon} = \frac{\Delta m g L}{A \Delta L}, \tag{1}$$

where $\Delta m/\Delta L$ is the linear slope determined from the plot acquired by LabView 4.0 software, L is the initial length of tube between grips, g is 9.81 m s^{-2} and A is the cross-sectional area of the tube. A was calculated by using equation (2), where the outside (OD) and inside (ID) diameters were measured at two 90° cross-sections per tube:

$$A = \pi \left[\left(\frac{\mathrm{OD}}{2} \right)^2 - \left(\frac{\mathrm{ID}}{2} \right)^2 \right]. \tag{2}$$

The moduli measured were statistically compared using one way ANOVA Tukey test (SigmaStat for Windows).

RESULTS AND DISCUSSION

Glass molds, modified with alkoxysilanes having a diversity of terminal functional groups, were used to synthesize PHEMA-MMA hydrogel tubes. We investigated the effect of silane modification of molds on the morphology and elastic modulus of PHEMA-MMA hydrogel tubes relative to those synthesized in unmodified molds.

Surface characterization of glass

As summarized in Table 1, the silane-glass modification reactions were successful for all three PEOSi, AminoSi and FluoroSi, as indicated by changes in surface elemental composition for both glass molds and coverslips. For example, for glass molds and coverslips modified with AminoSi, the presence of nitrogen indicates the success of this reaction; similarly, for glass molds and coverslips modified with FluoroSi, the presence of fluorine confirms the silane reaction with glass. Relative to unmodified glass coverslips, all modified coverslip surfaces exhibited a decrease in silicon, oxygen and sodium concentrations and an increase in carbon (except for Glass-FluoroSi). While we observed a substantial amount of adventitious carbon adsorbed on unmodified glass surfaces, this amount was similar to that reported by others [22]. All silane-modified glass molds and coverslips were transparent. The changes in dynamic advancing and receding water contact angle data confirmed the success of surface modification, where surfaces became more hydrophobic with silane modification relative to unmodified glass ($33^\circ/0^\circ$). As may be expected, Glass-FluoroSi surfaces were the most hydrophobic ($104^\circ/74^\circ$) followed by Glass-AminoSi ($97^\circ/35^\circ$) and Glass-PEOSi ($47^\circ/38^\circ$). The large hysteresis observed for

Table 1.
Un-modified and silane-modified glass surfaces characterized by XPS (at 20° take-off angle) and dynamic advancing (θ_a) and receding (θ_r) water contact angles (Wilhelmy plate method; $n = 3$)

Surface	Silane elemental composition	XPS elemental composition of glass mold surfaces	XPS elemental composition of glass coverslip surfaces	Contact angle of glass coverslip surfaces (θ_a/θ_r)
Glass	$(SiO_2Na)_n$	$Si_{18.1}O_{43.7}C_{37.5}Na_{0.7}$	$Si_{19.4}O_{44.5}C_{33.8}Na_{2.2}$	$33^\circ \pm 0^\circ/0^\circ \pm 0^\circ$
Glass-PEOSi	$Si_1O_{11}C_{21}$	$Si_{22.9}O_{30.1}C_{47.0}Na_0$	$Si_{12.7}O_{29.9}C_{56.9}Na_{0.5}$	$47^\circ \pm 3^\circ/38^\circ \pm 2^\circ$
Glass-AminoSi	$Si_1O_3C_8N_2$	$Si_{18.1}O_{23.3}C_{55.5}Na_0N_{2.4}$	$Si_{9.7}O_{22.1}C_{62.9}Na_0N_{5.3}$[a]	$97^\circ \pm 7^\circ/35^\circ \pm 3^\circ$
Glass-FluoroSi	$Si_1O_3C_{14}F_{13}$	$Si_{11.4}O_{16.9}C_{35.8}Na_0F_{36.0}$	$Si_{15.5}O_{32.4}C_{23.2}Na_{1.4}F_{27.5}$	$104^\circ \pm 5^\circ/74^\circ \pm 20^\circ$

[a] Some samples were contaminated with chlorine, but this was not representative.

Glass-AminoSi surfaces may reflect chemical heterogeneity, roughness or a patchy overlayer [24].

To gain greater insight into the modified layer, the XPS data of glass coverslips (including data acquired at 90° take-off angle, but not shown), were used to calculate the fraction of surface coverage (f) and thickness of the overlayer (d) using the 'partial coverage' model [24]. We used sodium and its change in composition with modification to represent the underlying glass substrate. This model implies that the silane layer occupies an area fraction f on an infinite uniform substrate with an overlayer/substrate intensity ratio of:

$$\frac{I_{\mathrm{B}}}{I_{\mathrm{A}}} = \frac{f I_{\mathrm{Bo}}\{1 - \exp[-d/(\lambda_{\mathrm{B}} \sin\theta)]\}}{(1-f) I_{\mathrm{Ao}} + f I_{\mathrm{Ao}} \exp[-d/(\lambda_{\mathrm{B}} \sin\theta)]}, \tag{3}$$

where I_{B} is the intensity of an atomic species unique to the overlayer (carbon, nitrogen, or fluorine in our case), I_{Bo} represents the intensity of that particular element expected for a pure overlayer of an infinite thickness (i.e. the ratio of nitrogen atoms in an AminoSi molecule), I_{A} is the intensity of the sodium peak in the substrate, I_{Ao} represents the intensity of sodium measured in clean glass at a 90° take-off angle (the chemical species being present in the ratio Si/O/C/Na = 6 : 15 : 3 : 1), λ_B is the inelastic mean free path of that unique elemental species within the overlayer and θ is the angle measured between the photoelectrons ejected and the sample surface. This model assumes that for a value of $f = 0$ no silane layer is present on the analyzed surface, while for $f = 1$ a uniform overlayer thickness d is present on the glass.

Figure 1 summarizes the overlayer thickness and fraction coverage calculated for surface-modified coverslips. In order to better understand these data, we calculated

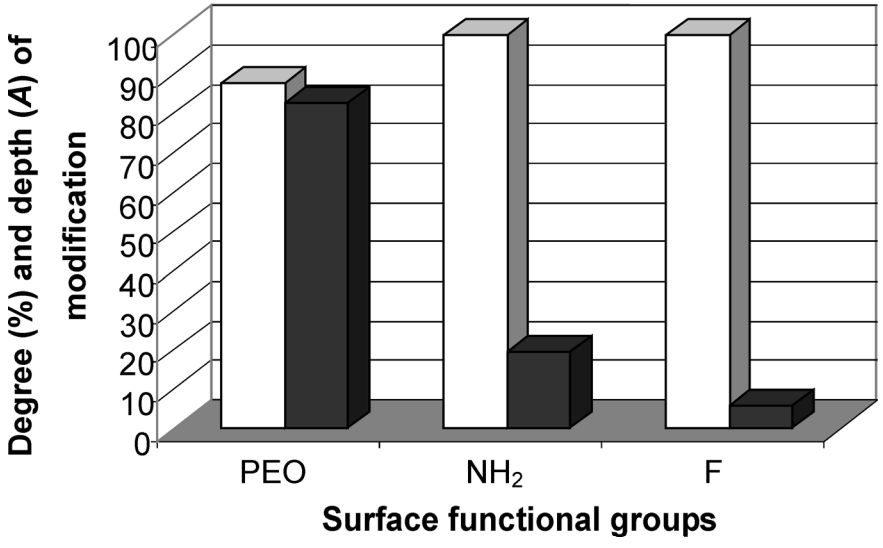

Figure 1. Surface coverage (□) and thickness (■) of silane layer on surface-modified glass coverslips.

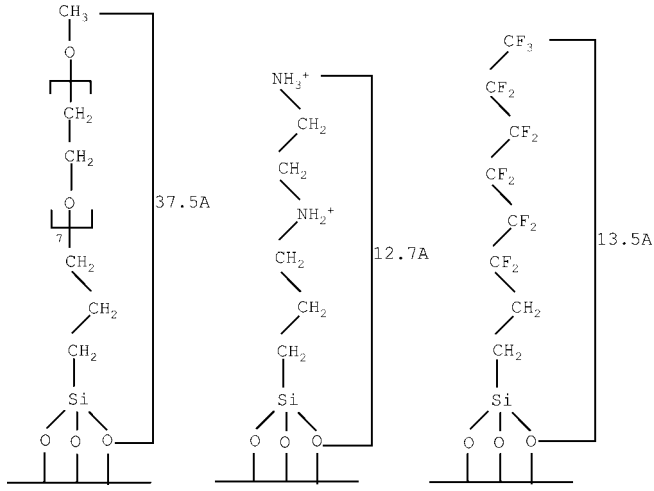

Figure 2. Trans-extended chain projections of the three silanes employed: PEOSi (left), AminoSi (middle) and FluoroSi (right).

the total molecular length of every silane based on the projected bond lengths of each silane, according to a published procedure [25]. As shown in Fig. 2, each structure is represented as a trans-extended chain projection with respect to the surface normal [26]. Combining the data in Fig. 1 with the theoretical extended conformational lengths of Fig. 2 provides better insight into the number of silane layers and their 'patchiness'. For Glass-PEOSi, where the extended conformation is 37.5 Å, surface coverage is 88% and thickness is 82.5 Å, there are likely more than 2 monolayers of patchy silane. For Glass-AminoSi, where the calculated extended conformation is 12.7 Å, surface coverage is 100% and thickness is 19.3 Å, there is likely a uniform coverage of almost 2 monolayers. Similarly, for Glass-FluoroSi, where the calculated extended conformation is 13.5 Å, surface coverage is 100% and thickness is 5.8 Å, there is likely patchy coverage with molecules oriented along (or collapsed on) the glass surface. The different conformations hypothesized for the different silanes may be explained by a spectrum of interactions between silanes and surfaces [21]. For example, the amine groups of AminoSi may hydrogen bond with free surface silanols, thereby providing an adsorbed conformation of trains and loops, whereas FluoroSi may have a predominantly train conformation due to weak acid–base interactions between the fluorosilane and glass.

Surface characterization of polymeric tubes

To assess the stability of the modified glass mold surface, we examined the PHEMA-MMA hydrogel tube surfaces for silane contamination by XPS. As summarized in Table 2, there is some evidence of silane on all hydrogel tubes; however, given that the greatest amount of silicon was observed on PHEMA-MMA tubes prepared in unmodified glass molds, the 'contamination' that we observed on PHEMA-MMA tubes made in silane-modified tubes is likely insignificant. The silicon mea-

Table 2.
XPS data (at 20° take-off angle) of hydrogel tubes prepared in unmodified and silane-modified glass molds

Surface	Silane elemental composition	XPS elemental composition of hydrogel tubes
Glass	$(SiO_2Na)_n$	$Si_{5.0}O_{25.5}C_{69.4}$
Glass-PEOSi	$Si_1O_{11}C_{21}$	$Si_{1.2}O_{28.2}C_{70.5}$
Glass-AminoSi	$Si_1O_3C_8N_2$	$Si_{1.7}O_{28.2}C_{70.1}$
Glass-FluoroSi	$Si_1O_3C_{14}F_{13}$	$Si_{1.2}O_{26}C_{65.2}F_{7.7}$

Table 3.
Tube dimensions ($n = 4$)

Mold	Inner diameter (μm)	Wall thickness (μm)	Gel thickness (μm)
Glass	2118 ± 212	511 ± 35	351 ± 24
Glass-PEOSi	2118 ± 102	561 ± 14	424 ± 11
Glass-AminoSi	2079 ± 102	558 ± 16	337 ± 9
Glass-FluoroSi	2043 ± 89	575 ± 9	354 ± 11

The outer diameter was equivalent for all tubes and equaled that of the inner diameter of the mold, which was 3400 μm.

sured is likely due to adventitious silicon in all cases, except for the PHEMA-MMA tubes prepared in Glass-FluoroSi molds, where significant fluorine was evident on PHEMA-MMA tubes. Overall, the results suggest that the silane-modified glass mold layer was stable during HEMA-MMA polymerization.

Tube-wall morphology

The inner and outer diameters at 90° cross-sections were measured for all tubes, as summarized in Table 3. As shown here and in the SEM micrographs of Fig. 3, all tubes were concentric and had a biphasic structure with an outer gel phase and an inner spongy phase. Both the wall thickness and gel-phase thickness were statistically the same for tubes synthesized in clean and surface-modified glass molds (cf., Table 3; $n = 4$, mean $\pm$ standard deviation). The mold surface chemistry influenced outer wall morphology: tubes prepared in unmodified tubes exhibited a 'cracked' outer wall structure described previously [8] whereas tubes prepared in modified molds had a smooth outer morphology (cf., Fig. 3c, 3f, 3i, 3l). Tubes prepared in unmodified glass molds appeared to have defects in the wall structure which resulted in the cracked morphology observed (cf., Fig. 3b). The difference in outer morphology may be related to mold surface properties where modified molds, that were more hydrophobic than unmodified molds, allowed hydrophobic MMA of P(HEMA-co-MMA) to spread more easily *vs.* unmodified molds where the MMA may have beaded. Wall morphology influences the physical properties of the tubes, including both diffusion across the tube wall [7] and overall modulus of the tube. As

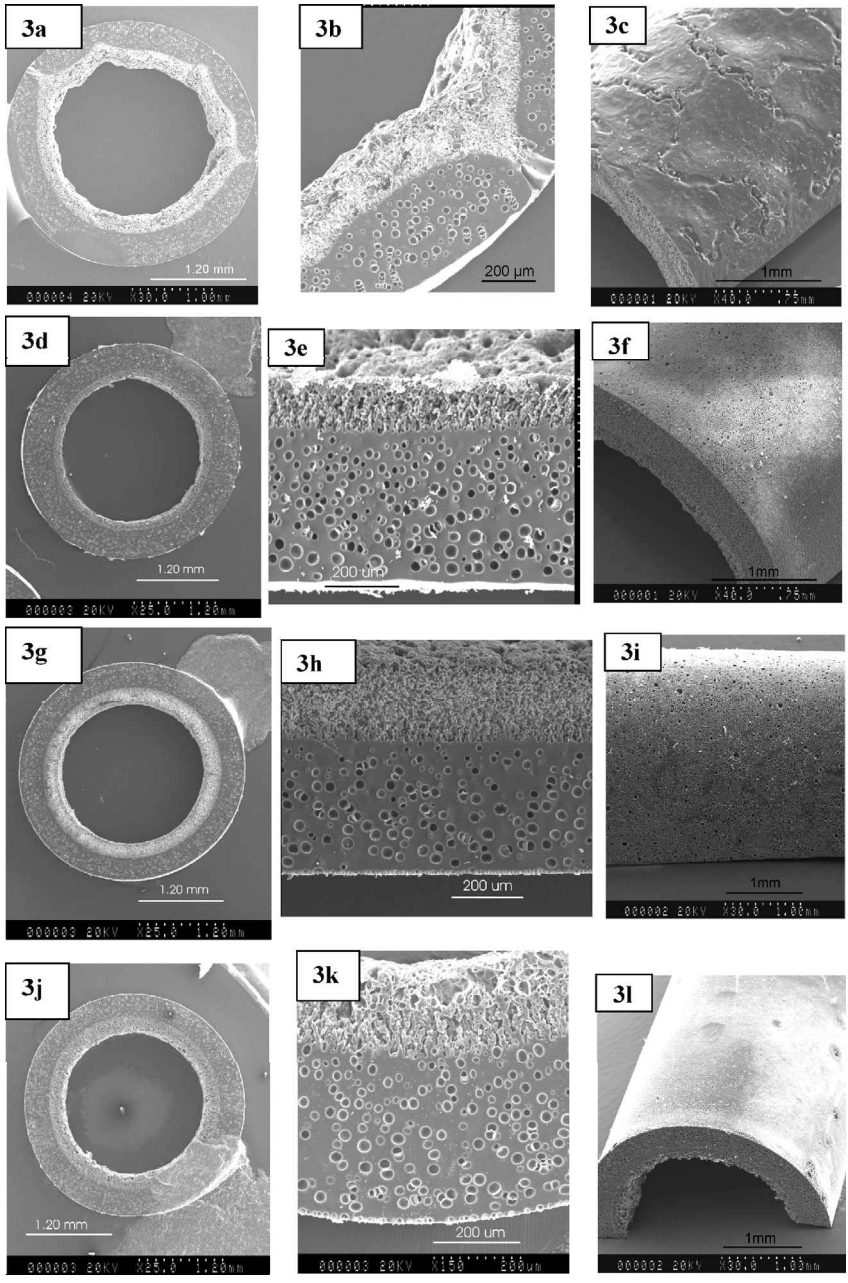

Figure 3. SEM micrographs of hydrogel tubes (cross-sections of tubes, tube walls and outer surface) synthesized in molds with glass. (a, b, c) Unmodified, (d, e, f) modified with PEOSi, (g, h, i) modified with AminoSi and (j, k, l) modified with FluoroSi.

described below, tube morphology was investigated and correlated with mechanical properties.

Qualitative comparison of hydrogel tube release from glass molds

While there are quantitative methods to determine adhesion of films on different substrates, including for example, the 180° peel test [27], the adhesion test [28] and the T-peel test [29], we assessed release qualitatively because our hydrogel tubes are weak and tear easily under applied force, making them unsuitable for the quantitative methods available for tubular shapes [30]. The release from glass molds was scored from most difficult to easiest, with release being most difficult from FluoroSi molds, followed by unmodified molds and easiest from AminoSi and PEOSi molds. Since the best release was obtained from Glass-PEOSi and Glass-AminoSi molds, only these two types of hydrogel tubes were further characterized for modulus.

While Glass-FluoroSi was the most hydrophobic, release was the most difficult, which may seem counter-intuitive because poor wetting (i.e. poor adhesion) is often observed when the surface tension of a liquid is larger than the critical surface tension (γ_c) of a surface [23], as in this case (cf., contact angle data in Table 1). The acid–base interactions between surface and polymer may also influence adhesion [31], where, for example, Glass-FluoroSi surfaces are basic and PHEMA-MMA is acidic. The poor release observed from Glass-FluoroSi molds may also be explained by hydrophobic–hydrophobic interactions between hydrophobic PHEMA-MMA and hydrophobic Glass-FluoroSi surfaces. This interaction between the hydrogel tube and glass mold may have been strengthened by fluorocarbon adsorbed onto PHEMA-MMA surfaces, as was evidenced by XPS data.

Mechanical properties of hydrogel tubes

Given the better release ability of tubes from Glass-PEOSi and Glass-Amino modified molds, only these tubes were further examined for mechanical properties relative to tubes synthesized in unmodified glass molds. A correlation between wall morphology and elastic modulus is well accepted [8], with the gel phase being responsible for mechanical properties. While the thickness of the gel phase in the continuous areas of the tube wall for tubes made in unmodified molds was similar to that of tubes synthesized in silane-modified molds, there was a difference in modulus measured, which may be explained by the difference in tube-wall morphology. The disruption of the layer structure, which is known to give mechanical strength to laminates, by intrusion of the spongy layer into the gel one, may account for the lower Young's modulus of 191 ± 38.5 kPa measured for PHEMA-MMA tubes synthesized in unmodified glass molds vs. those tubes synthesized in molds modified with Glass-PEOSi (734 ± 5 kPa) or Glass-AminoSi (818 ± 158 kPa). While elastic moduli of tubes synthesized in Glass-PEOSi

and Glass-AminoSi molds were statistically the same, those of tubes made in unmodified glass molds were statistically different ($P < 0.005$).

CONCLUSIONS

Silane modification of glass molds affected release and modulus of PHEMA-MMA hydrogel tubes. Release was facilitated and modulus increased for PHEMA-MMA tubes synthesized in Glass-PEOSi and Glass-AminoSi tubes *vs.* unmodified glass molds, likely due to the increased hydrophobicity associated with these silane-modified surfaces; however, the same was not true for Glass-FluoroSi, perhaps due to the oleophobic nature of the fluorinated compound. These modified glass molds produced hydrogel tubes with wall morphologies having a continuous, two-layer structure, which consequently enhanced the tensile strength of tubes. These tubes are currently being assessed for their regenerative capacity of both peripheral nerve and spinal cord tissue.

Acknowledgements

We are grateful to Dr. Rana Sodhi for his advice on XPS analysis, to Alex Goraltchouk for technical assistance and to the Natural Sciences and Engineering Research Council and the University of Toronto Scholarship program for partial funding of this project.

REFERENCES

1. J. D. Andrade (Ed.), *Hydrogels for Medical and Related Applications, ACS Symposium Series, Volume 31.* American Chemical Society, Washington, DC (1976).
2. N. A. Peppas, *Hydrogels in Medicine and Pharmacy, Volumes 1–3.* CRC Press, Boca Raton, FL (1987).
3. A. Loebsack, K. Greene, S. Wyatt, C. Culberson, C. Austin, R. Beiler, W. Roland, P. Eiselt, J. Rowley, K. Burg, D. Mooney, W. Holder and C. Halberstadt, *J. Biomed. Mater. Res.* **57**, 575 (2001).
4. R. Midha, M. S. Shoichet, P. D. Dalton, X. Cao, C. A. Munro, J. Noble and M. K. K. Wong, *Transplant. Proc.* **33**, 612 (2001).
5. E. C. Tsai, A. Parr, P. D. Dalton, M. S. Shoichet and C. H. Tator, Regeneration of adult brainstem motor axons after complete spinal cord transection with novel synthetic hydrogel quidance channels. Society for Neuroscience (2003) (Abstract).
6. P. D. Dalton, E. Tsai, R. L.Van Bendegem, C. H. Tator and M. S. Shoichet, *Hydrogel Nerve Guides Promote Regeneration in the Central Nervous System.* Society for Biomaterials, Tampa Bay, FL (2002).
7. Y. Luo, P. D. Dalton and M. S. Shoichet, *Chem. Mater.* **13**, 4087 (2001).
8. P. D. Dalton, L. Flynn and M. S. Shoichet, *Biomaterials* **23**, 3843 (2002).
9. P. D. Dalton and M. S. Shoichet, *Biomaterials* **22**, 2661 (2001).
10. A. J. Shields, D. M. Hepburn, I. J. Kemp and T. M. Cooper, *Polymer Degrad. Stabil.* **70**, 253 (2000).

11. B. J. Briscoe and S. S. Panesar, *J. Phys. D Appl. Phys.* **19**, 841 (1986).
12. E. P. Singh and R. Subramanian, US Patent No. 5,204,126 (1993).
13. S. Hirotoshi, N. Yasushi, Y. Masayuki and K. Masato, US Patent No. 5,804,674 (1998).
14. H. Hosokawa, J. Maeshima and F. Suto, EP Patent No. 771629 (1997).
15. J. Travis and C. Baird, *Plastics Design Process.* **23**, 11 (1983).
16. M.-F. Vallat, J. Schultz, C. Mauzac and M. Jacquin, *Polym. Adv. Technol.* **10**, 237 (1999).
17. W. R. Willkomm, R. M. Jennings and C. W. Macosko, *Plastics Rubber Composit. Process. Appl.* **19**, 69 (1993).
18. L. H. Wadhwa and A. M. Steurer, EP Patent No. 0330488 (1989).
19. Y. M. Yuan and M. S. Shoichet, *Macromolecules* **33**, 4926 (2000).
20. Y. W. Tang, J. P. Santerre, R. S. Labow and D. G. Taylor, *J. Biomed. Mater. Res.* **35**, 371 (1997).
21. E. P. Plueddemann, *Silane Coupling Agents.* Plenum Press, New York, NY (1982).
22. S. Saneinejad and M. S. Shoichet, *J. Biomed. Mater. Res.* **42**, 13 (1998).
23. B. Arkles, *Chemtech* **7**, 766 (1977).
24. J. Andrade (Ed.), *Surfaces and Interfacial Aspects of Biomedical Polymers, Volume 1.* Plenum, New York, NY (1985).
25. B. Lom, K. E. Healy and P. E. Hockberger, *J. Neurosci. Methods* **50**, 385 (1993).
26. *CRC Handbook of Chemistry and Physics*, 3rd electronic edn, pp. 9-1–9-14. CRC Press, Boca Raton, FL (1999).
27. J. K. Kim, W. H. Kim and D. H. Lee, *Polymer* **43**, 5005 (2002).
28. C. R. Park and D. L. Munday, *Int. J. Pharm.* **237**, 215 (2002).
29. F. Aran-Ais, A. M. Torro-Palau, A. C. Orgiles-Barcelo, and J. M. Martin-Martinez, *J. Adhesion Sci. Technol.* **16**, 1431 (2002).
30. W. R. Willkomm, R. M. Jennings and C. W. Macosko, *Plastics Rubber Composit. Process. Appl.* **19**, 69 (1993).
31. F. M. Fowkes, in: *Surface and Interfacial Aspects of Biomedical Polymers, Volume 1*, J. D. Andrade (Ed.), pp. 337–372. Plenum, New York, NY (1985).